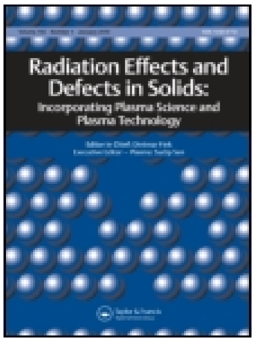

Taylor & Francis
Taylor & Francis Group

Radiation Effects and Defects in Solids

Incorporating Plasma Science and Plasma Technology

ISSN: 1042-0150 (Print) 1029-4953 (Online) Journal homepage: http://www.tandfonline.com/loi/grad20

Role of the orientation angles of reacting nuclei in evaporation residue production

G. Mandaglio , M. Manganaro , G. Fazio , G. Giardina , C. Saccá , A. I. Muminov & A. K. Nasirov

To cite this article: G. Mandaglio , M. Manganaro , G. Fazio , G. Giardina , C. Saccá , A. I. Muminov & A. K. Nasirov (2009) Role of the orientation angles of reacting nuclei in evaporation residue production, Radiation Effects and Defects in Solids, 164:5-6, 287-290, DOI: 10.1080/10420150902805021

To link to this article: https://doi.org/10.1080/10420150902805021

Published online: 01 Dec 2010.

Radiation Effects & Defects in Solids
Vol. 164, Nos. 5–6, May–June 2009, 287–290

Role of the orientation angles of reacting nuclei in evaporation residue production

G. Mandaglio[a]*, M. Manganaro[a], G. Fazio[a], G. Giardina[a], C. Saccá[b], A.I. Muminov[c] and A.K. Nasirov[c,d]

[a] *INFN, Sezione di Catania, and Dipartimento di Fisica dell'Universitá di Messina, 98166 Messina, Italy;* [b] *Dipartimento di Scienze della Terra, Universitá di Messina, 98166 Messina, Italy;* [c] *Heavy Ion Physics Department, Institute of Nuclear Physics, 702132 Tashkent, Uzbekistan;* [d] *Flerov Laboratory of Nuclear Reactions, JINR, 141980 Dubna, Russia*

(*Received 24 May 2008; final version received 8 February 2009*)

The influence of the orientation angles of the projectile- and target-nucleus symmetry axes relative to the beam direction on the production of the evaporation residues (ERs) is investigated for the ^{48}Ca+^{154}Sm reaction as a function of the beam energy. The measured yields of ERs by massive nuclei reactions have been well reproduced by using the partial fusion and quasi-fission cross-sections obtained in the dinuclear system model. At lower beam energies, only the orientation angles close to $\alpha_P = 30°$ (projectile) to $\alpha_P = 0°–15°$(target) can contribute to the ER formation. At large beam energies (about $E_{c.m.} = 140–180$ MeV), all $\alpha_P - \alpha_T$ configurations of reactants can contribute to the ER cross-section, which ranges between 10 and 100 mb, while at $E_{c.m.} > 185$ MeV, the ER cross-section ranges between 1 and 0.1 mb because the fission barrier for the compound nucleus decreases by increasing its excitation energy and angular momentum.

Keywords: heavy ion reaction; fusion; quasi-fission; evaporation residues; orientation of reactants

PACS: 25.70.Jj; 25.70.Gh; 25.70.Lm; 25.85.Ge

We use the method developed in our previous papers (*1–4*) to describe the role of all three stages, starting from the dinuclear system (DNS) formation (*5*) at capture of the projectile by the target nucleus, then its evolution into a compound nucleus and the production of the evaporation residues (ERs) after the emission of gamma-quanta, neutrons, protons and α-particles. The method allows us to determine the corresponding cross-sections of capture, complete fusion and the formation of the ERs. By this method, we were able to determine the angular momentum distribution of the crosssection at the DNS stage (determined by the conditions of the entrance channel) and at competition between quasi-fission and complete fusion, affected by the conditions of the reaction mechanism. Therefore, the de-excitation chain of the compound nucleus (characterized by the fission-evaporation competition) is also affected by the reaction dynamics (*6, 7*). The cross-section of ERs, which can be compared with the corresponding experimental data, is calculated by the determination of the survived $^{A_{CN}}Z_{CN}$ compound nucleus and other excited intermediate nuclei

*Corresponding author. Email: gmandaglio@unime.it

ISSN 1042-0150 print/ISSN 1029-4953 online

DOI: 10.1080/10420150902805021
http://www.informaworld.com

along the de-excitation cascade of CN after the emission of neutrons, y protons and k α-particles at the xth step of the cascade by the formula (*6*, *8*):

$$\sigma_{\mathrm{ER}(x)}(E_x^*) = \sum_{\ell=0}^{\ell_d}(2\ell+1)\sigma^{\ell}_{(x-1)}(E_x^*)W_{\mathrm{sur}(x-1)}(E_x^*, \ell). \tag{1}$$

In our model, we calculate $\sigma^{\ell}_{\mathrm{fus}}(E^*_{\mathrm{CN}})$ by estimating the competition of the complete fusion with quasi-fission if we know the partial capture cross-section:

$$\sigma^{\ell}_{\mathrm{fus}}(E_{\mathrm{c.m.}}) = \sigma^{\ell}_{\mathrm{cap}}(E_{\mathrm{c.m.}})P_{\mathrm{CN}}(E_{\mathrm{c.m.}}, \ell), \tag{2}$$

where $P_{\mathrm{CN}}(E_{\mathrm{c.m.}})$ is the hindrance factor for the formation of the compound nucleus connected with the competition between complete fusion and quasi-fission as possible channels of evolution of the DNS. Details of the method to calculate $\sigma^{\ell}_{\mathrm{cap}}$ and $\sigma^{\ell}_{\mathrm{fus}}$ are described in (*8*, *9*).

The present paper is devoted to the study of the dependence of the ER cross-section on the orientation angles of the deformed nuclei. Certainly, it is impossible to directly establish the above-mentioned dependence in an experimental way. But theoretical analysis allows us to estimate the contributions of collisions by different orientation angles to the measured ER cross-sections.

Usually, the final results of the ER cross-sections are obtained by averaging the contributions calculated for the different orientation angles of the symmetry axis of the reacting nuclei

$$\langle\sigma_{ER}(E_{\mathrm{c.m.}})\rangle = \int_0^{\pi/2}\sin\alpha_{\mathrm{P}}\int_0^{\pi/2}\sigma_{\mathrm{ER}}(E_{\mathrm{c.m.}};\alpha_{\mathrm{P}},\alpha_{\mathrm{T}}))\sin\alpha_{\mathrm{T}}\,d\alpha_{\mathrm{P}}\,d\alpha_{\mathrm{T}}, \tag{3}$$

where $\sigma_{\mathrm{ER}}(E_{\mathrm{c.m.}};\alpha_{\mathrm{P}},\alpha_{\mathrm{T}})$ is calculated by Equation (1) for all considered orientation angles of the symmetry axes of the projectile and target nuclei. The fusion excitation function is determined by the product of the partial capture cross-sections $\sigma^{\ell}_{\mathrm{cap}}$ and fusion probabilities P_{CN} of DNS:

$$\sigma_{\mathrm{fus}}(E;\alpha_{\mathrm{P}},\alpha_{\mathrm{T}}) = \sum_{\ell=0}^{\ell_d}(2\ell+1)\sigma_{\mathrm{cap}}(E,\ell;\alpha_{\mathrm{P}},\alpha_{\mathrm{T}})P_{\mathrm{CN}}(E,\ell;\alpha_{\mathrm{P}},\alpha_{\mathrm{T}}). \tag{4}$$

The fission cross-section is calculated by the advanced statistical code (*8*, *10*) that takes into account the damping of the shell correction in the fission barrier as a function of the nuclear temperature and orbital angular momentum. Instead, fast fission is a binary process that occurs only at high values of the orbital angular momentum. It consists of the disintegration of the mononucleus into two fragments, which has a very high angular momentum and survives quasi-fission (the decay of the DNS into two fragments). Moreover, it is well known that the fission barrier for a compound nucleus decreases by increasing its angular momentum and disappears at the definite value ℓ_f (*11*). Therefore, the mononucleus, having a high value of angular momentum, splits into two fragments immediately if its angular momentum is larger than ℓ_f, because there is not a barrier providing stability.

To investigate the influence of the angular orientations of the projectile and target nuclei on the ER yields, we chose the ^{48}Ca+^{154}Sm reaction because the experimental data of the ER cross-sections for this reaction are presented in (*12*). To understand in detail the preceding mechanism leading to the formation of the ER, we studied the dependence of the competition between quasi-fission and complete fusion on the orientation angles α_{P} and α_{T} of the symmetry axes of the projectile and target nuclei, respectively. The quadrupole deformation parameter of ^{154}Sm is equal to 0.27 in the ground state. Although ^{48}Ca is spherical, in our calculations we took into account the quadrupole 2^+ and octupole 3^- collective excitations and used for it the values $\langle\beta_2^{(+)}\rangle = 0.101$ (from (*13*)) and $\langle\beta_3^{(-)}\rangle = 0.25$ (from (*14*)) as the effective deformation parameters. The ER data

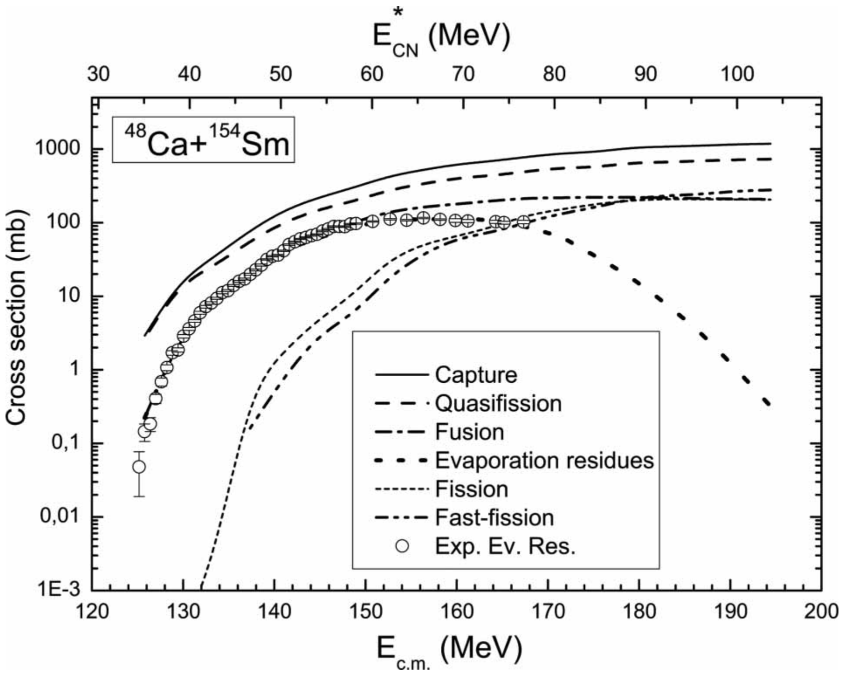

Figure 1. The theoretical excitation functions for capture (solid line), fusion + fast-fission (dot-dashed line), quasi-fission (dashed line), ER (thick short dashed line), fission (thin short-dashed line) and fast-fission (dash-double dotted line) versus the beam energy $E_{\mathrm{c.m.}}$ for the ^{48}Ca+^{154}Sm reaction leading to the ^{202}Pb compound nucleus. Open circles are the experimental data of the ERs given in (*12*).

are comparable with the fusion cross-section at beam energies lower than $E_{\mathrm{c.m.}} = 150$ MeV, whereas at beam energies higher than $E_{\mathrm{c.m.}} = 160$ MeV, the fission cross-section overcomes the ERs, becoming comparable with the fusion cross-section (Figure 1).

At beam energies lower than about $E_{\mathrm{c.m.}} = 140$ MeV, the quasi-fission contribution is comparable with the capture formation, and the fusion process is strongly hindered. Therefore, only the small orientation angles of the symmetry axis of the projectile–target nuclei relative to the beam direction give appreciable contributions to the fusion cross-section.

This phenomenon was discussed in (*9*), and we observe it clearly for the investigated ^{48}Ca+^{154}Sm reaction. This is related to the dependence of the potential energy surface, particularly of the driving potential $U_{\mathrm{d}r}$, on the orientation angles. As a result, the competition between complete fusion and quasi-fission becomes a function of α_{P} and α_{T} (*9*).

The dependence of the production of the ER nuclei on the orientation angle α_{T} of the target-nucleus symmetry axis is presented in Figure 2 for some values of the beam energy and the orientation angle α_{P} of the projectile symmetry axis. In the figure, the different lines are related to various values of α_{P}. At the smallest beam energy $E_{\mathrm{c.m.}} = 125.8$ MeV (corresponding to $E_{\mathrm{c.m.}} =$ 35.1 MeV of the compound nucleus), we observe the ER cross-section only for $\alpha_{\mathrm{P}} = 30°$ and $\alpha_{\mathrm{T}} =$ 0°–12° range. At $E_{\mathrm{c.m.}} = 137.2$ MeV ($E_{\mathrm{c.m.}} = 46.5$ MeV), the number of orientations contributing to the ER production increases, and we obtain observable results for $\alpha_{\mathrm{P}} = 0°$, 30°, 60°, 90° in the ranges of the α_{T} orientations from 0° up to 59°, 58°, 28° and 13°, respectively, because in the collisions with the corresponding beam energies, capture and complete fusion are impossible at larger values of the orientation angle α_{T} . Therefore, when the beam energy is high enough (for example, $E_{\mathrm{c.m.}} = 156.3$ MeV or $E_{\mathrm{c.m.}} = 171.2$ MeV, corresponding to $E_{\mathrm{c.m.}} = 65.6$ or 80.8 MeV respectively), all angular configurations of reactants lead to the observation of the ERs with cross-sections in the range 10–100 mb. At $E_{\mathrm{c.m.}} = 194.4$ MeV ($E_{\mathrm{c.m.}} = 103.7$ MeV), all orientation

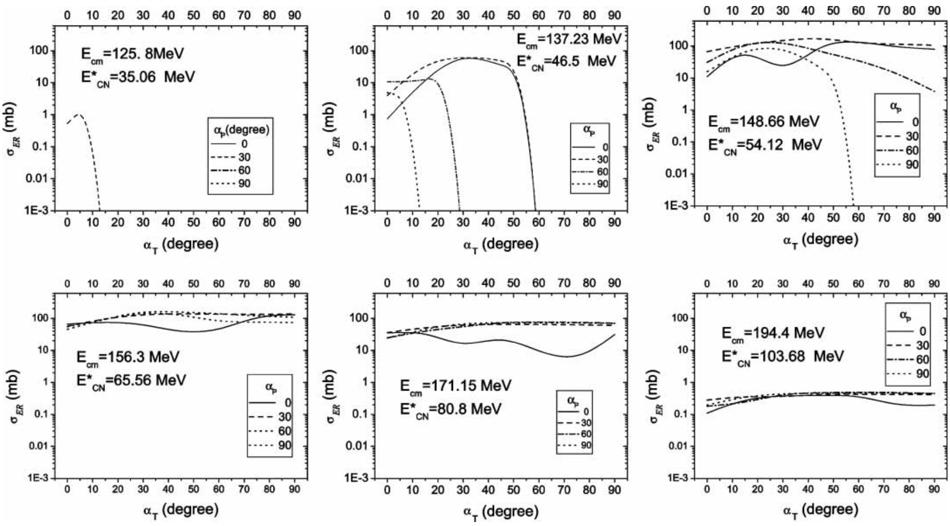

Figure 2. ER cross-section versus the α_T orientation angle, at some fixed energies $E_{c.m.}$ and for a set of α_P orientation angles.

angles can contribute to the formation of ERs, but with small cross-sections, $\sigma_{ER} = 1\text{–}0.1$ mb, because by increasing the beam energy, the number of partial waves leading to the complete fusion increases. The decrease of σ_{ER} at $E_{c.m.} = 194.4$ MeV is related to the fact that the fission barrier for a compound nucleus decreases by increasing its excitation energy (*3*, *4*) and angular momentum (*11*). Therefore, the survival probability of the heated compound nucleus along the de-excitation cascade decreases. Another phenomenon leading to the decrease of σ_{ER} at higher beam energy is the fast-fission process.

References

(1) Giardina, G.; Hofmann, S.; Muminov, A.I.; Nasirov, A.K. *Eur. Phys. J. A* **2000,** *8,* 205–216.
(2) Giardina, G.; Hanappe, F.; Muminov, A.I.; Nasirov, A.K.; Stuttge, L. *Nucl. Phys. A* **2000,** *671,* 165–188.
(3) Fazio, G.; Giardina, G.; Lamberto, A.; Ruggeri, R.; Saccá, C.; Palamara, R.; Muminov, A.I.; Nasirov, A.K.; Yakhshiev, U.T.; Hanappe, F.; Materna, T.; Stuttge, L. *Eur. Phys. J. A* **2004,** *19,* 89–104.
(4) Fazio, G.; Giardina, G.; Lamberto, A.; Ruggeri, R.; Saccá, C.; Palamara, R.; Muminov, A.I.; Nasirov, A.K.; Yakhshiev, U.T.; Hanappe, F.; Materna, T.; Stuttge, L. *J. Phys. Soc. Jpn.* **2003,** *72,* 2509–2522.
(5) Adamian, G.G.; Antonenko, N.V.; Scheid, W.; Volkov, V.V. *Nucl. Phys. A* **1998,** *633,* 409–420.
(6) Fazio, G.; Giardina, G.; Lamberto, A.; Muminov, A.I.; Nasirov, A.K.; Hanappe, F.; Materna, T.; Stuttge, L. *Eur. Phys. J. A* **2004,** *22,* 75–87.
(7) Nasirov, A.K.; Giardina, G.; Muminov, A.I.; Scheid, W.; Yakhshiev, U.T. In Proc. of the Symposium on Nuclear Cluster, Rauischolzhausen, Germany, Jolos, R.V., and Scheid, W. Eds. 2003, EP Systema, Debrecen, 2002, 415–426; Nasirov, A.K.; Giardina, G.; Muminov, A.I.; Scheid, W.; Yakhshiev, U.T. *Acta Phys. Hung. A* **2004,** *19,* 109–120.
(8) Fazio, G.; Giardina, G.; Mandaglio, G.; Hanappe, F.; Muminov, A.I.; Nasirov, A.K.; Scheid, W.; Stuttge, L. *Mod. Phys. Lett. A* **2005,** *20,* 391–405.
(9) Nasirov, A.K.; Fukushima, A.: Toyoshima, Y.; Aritomo, Y.; Muminov, A.; Kalandarov, S.; Utamuratov, R. *Nucl. Phys. A* **2005,** *759,* 342–369.
(10) D'Arrigo A.; Giardina, G.; Herman, H.; Taccone, A. *Phys. Rev. C* **1992,** *46,* 1437–1444.
(11) Sierk, A.J. *Phys. Rev. C* **1986,** *33,* 2039–2053.
(12) Stefanini, A. M.; Trotta, M.; Behera, B.R.; Corradi, L.; Fioretto, E.; Gadea, A.; Latina, A.; Szilner, S.; Wu, Y.W.; Beghini, S.; Montagnoli, G.; Scarlassara, F.; Chizhov, A. Yu.; Itkis, I.M.; Kondratiev, N.A.; Pokrovskiy, I.V.; Sagaidak, R.N.; Kniajeva, G.N.; Kozulin, E.M.; Voskressensky, V.M.; Courtin, S.; Haas, F.; Rowley, N. *Eur. Phys. J. A* **2005,** *23,* 473–480.
(13) Raman, S.; Malarkey, C.H.; Milner, W.T.; Nestor, C.W.; Stelson, P.H. *At. Data Nucl. Data Tables* **1987,** *36,* 1–96.
(14) Spear, R.H. *At. Data Nucl. Data Tables* **1989,** *42*(1), 55–104.